Biochemistry

pubs.acs.org/biochemistry Article

Characterization of an *Acinetobacter baumannii* Monofunctional Phosphomethylpyrimidine Kinase That Is Inhibited by Pyridoxal Phosphate

Humberto De Vitto,[⋈] Kafi Belfon,[⋈] Nandini Sharma, Sarah Toay, Jan Abendroth, David. M. Dranow, Christine M. Lukacs, Ryan Choi, Hannah S. Udell, Sydney Willis, George Barrera, Olive Beyer, Teng Da Li, Katherine A. Hicks, Andrew T. Torelli, and Jarrod B. French*

Cite This: https://doi.org/10.1021/acs.biochem.3c00640 Read Online

ACCESS | Metrics & More | Article Recommendations | Supporting Information

ABSTRACT: Thiamin and its phosphate derivatives are ubiquitous molecules involved as essential cofactors in many cellular processes. The *de novo* biosynthesis of thiamin employs the parallel synthesis of 4-methyl-5-(2-hydroxyethyl)thiazole (THZ-P) and 4-amino-2-methyl-5(diphosphooxymethyl) pyrimidine (HMP) pyrophosphate (HMP-PP), which are coupled to generate thiamin phosphate. Most organisms that can biosynthesize thiamin employ a kinase (HMPK or ThiD) to generate HMP-PP. In nearly all cases, this enzyme is bifunctional and can also salvage free HMP, producing HMP-P, the monophosphate precursor of HMP-PP. Here we present high-resolution crystal structures of an HMPK from *Acinetobacter baumannii* (AbHMPK), both unliganded and with pyridoxal 5-phosphate (PLP) noncovalently bound. Despite the similarity between HMPK and pyridoxal kinase enzymes, our kinetics analysis indicates that AbHMPK accepts HMP exclusively as a substrate and cannot turn over pyridoxal, pyridoxamine, or pyridoxine nor does it display phosphatase activity. PLP does, however, act as a weak inhibitor of AbHMPK with an IC_{50} of 768 μM. Surprisingly, unlike other HMPKs, AbHMPK catalyzes only the phosphorylation of HMP and does not generate the diphosphate HMP-PP. This suggests that an additional kinase is present in *A. baumannii*, or an alternative mechanism is in operation to complete the biosynthesis of thiamin.

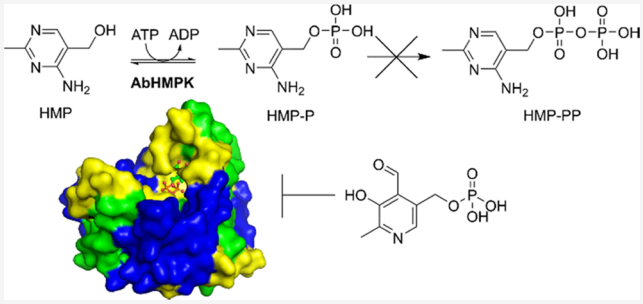

■ INTRODUCTION

Thiamin (vitamin B_1), is an essential nutrient that cannot be synthesized by humans and, thus, must come from dietary sources.[1,2] Its derivatives, particularly thiamin pyrophosphate, act as coenzymes for numerous cellular processes.[1,3] In all organisms that can biosynthesize thiamin, a convergent synthetic approach is employed whereby the thiazole and pyrimidine moieties, generated separately, are coupled by a thiamin phosphate synthase.[1,3−6] The pyrimidine precursor, 4-amino-2-methyl-5(diphosphooxymethyl)pyrimidine, also known as hydroxymethyl pyrimidine diphosphate (HMP-PP) is formed from the purine biosynthetic intermediate 5-aminoimidazole ribotide (AIR) through the action of two enzymes, ThiC, which generates the monophosphate (HMP-P) through a rearrangement reaction, and ThiD, a kinase that transfers the phosphate of ATP to HMP-P to yield the HMP-PP final product (Figure 1).[3,4,7] ThiD, also known as an hydroxylmethyl pyrimidine kinase (HMPK, EC 2.7.4.7) or HMP-P kinase (HMPPK) is reported to be bifunctional and also accepts HMP as a substrate (Figure 1) in order to salvage HMP.[3,7−10]

HMPK belongs to the ribokinase-like superfamily, a group that includes the carbohydrate kinase PfkB and the pyridoxal kinase family of proteins. Pyridoxal kinase (PLK) is an enzyme that converts pyridoxal, and various derivatives, into the ubiquitous coenzyme pyridoxal phosphate (PLP).[11−14] Not surprisingly considering the structural similarities of the substrates, a class of PLK/HMPK-like enzymes, that can catalyze either the phosphorylation of pyridoxal or HMP, have been identified (EC 2.7.1.49).[8,15,16] These enzymes are reported to convert HMP to HMP-P, but cannot catalyze phosphorylation of HMP-P. These proteins are proposed to have a common evolutionary ancestor that may explain some of the functional overlap.[11]

Here, we describe the unliganded and PLP-bound X-ray crystal structures of a putative HMPK from *Acinetobacter*

Received: November 15, 2023
Revised: January 12, 2024
Accepted: January 16, 2024

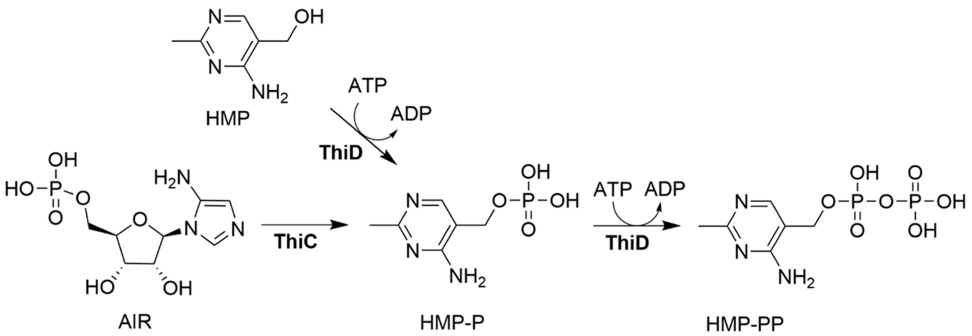

Figure 1. Reactions catalyzed by ThiD (HMPK) and ThiC. Hydroxymethyl pyrimidine kinase (HMPK) is a component of the thiamin biosynthesis pathway that salvages HMP, generating the phosphorylated product HMP-P. This product can also be made from the purine biosynthetic intermediate 5-aminoimidazole ribotide (AIR) using ThiC. The final pyrophosphate product, HMP-PP, is typically generated by a second phosphorylation reaction catalyzed by the same ThiD (HMPK) enzyme.

baumannii (AbHMPK). Sequence comparison suggests that this protein is an HMPK, however, the liganded structure shows clear density for the PLP in the active site, indicating that this enzyme can engage with this molecule. AbHMPK exhibits reasonable kinetics for HMP and does not turn over pyridoxal, pyridoxamine, or pyridoxine. Despite its selectivity for HMP(P) over pyridoxal and its derivatives, AbHMPK is inhibited by PLP at high micromolar concentrations, suggesting the possible coordinated regulation of thiamin and PLP biosynthesis in *A. baumannii*. Interestingly, this enzyme only uses one equivalent of ATP, and under the conditions that we tested the enzyme, produces only the monophosphorylated product, HMP-P. This suggests that this organism requires an additional enzyme, or uses an alternative pathway, to complete the synthesis of HMP-PP, a critical precursor for the biosynthesis of thiamine.

■ MATERIALS AND METHODS

Protein Expression and Purification. Cloning, expression, and purification followed standard protocols as previously described.[17−19] The gene for *A. baumanii* phosphomethylpyrimidine kinase was amplified from genomic DNA and cloned into the expression vector pBG1861 using ligation-independent cloning.[20] The expression vector provides a noncleavable N-terminal His_6-tag (SSGCID target ID AcaC.00867.a, SSGCID construct ID AcbaC.00867.a.B1, SSGCID batch AcbaC.00867.a.B1.PW37632). The gene was expressed in *Escherichia coli* BL21(DE3) Rosetta (Structural Genomics Consortium SGC, Toronto; with pRARE plasmid) following standard SSGCID protocols as described previously.[18] Purification was done using Ni-NTA affinity and size exclusion chromatography following standard SSGCID protocols.[17] The purified protein was concentrated to 22 mg/mL in its final buffer (25 mM HEPES pH 7.0, 500 mM NaCl, 5% glycerol, 2 mM DTT, 0.025% NaN_3), flash frozen in liquid nitrogen, and stored at −80 °C. This batch yielded 40 mg of purified protein from a starting culture of 2 L.

Crystallization, Data Collection, and Structure Solution. Crystals of *apo Acinetobacter baumannii* phosphomethylpyrimidine kinase were grown by mixing 0.4 μL of protein at 22 mg/mL, with 0.4 μL of reservoir of sparse matrix screen MCSG1 (Microlytics) condition C8 (200 mM ammonium sulfate, 100 mM sodium citrate/HCl pH 5.6, 25% (w/v) PEG 4000), in MRC2 sitting drop crystallization trays (SwisSci) with 50 μL reservoir volume. For the PLP-bound structure, crystals were then soaked overnight in reservoir solution supplemented with 5 mM pyridoxal phosphate. Both apo and PLP-bound crystals were cryoprotected with a mix of 20% (v/v) ethylene glycol and reservoir solution or soak solution, respectively. Crystals were then vitrified in liquid nitrogen. X-ray diffraction data for the apo crystal were collected at the APS beamline 21-ID-G on a Rayonix MX-300 CCD detector, while diffraction data for the PLP-bound sample were collected on a Rigaku FR-E+ rotating anode using Cu Kα radiation and a Rigaku Saturn 944+ CCD detector. The apo structure was solved by molecular replacement with the programs Balbes and Phaser using PDB entry 4C5L[16] as the search model. The PLP-bound structure was solved via Molecular replacement using the apo structure. Iterative manual real space model building using COOT[21] and reciprocal space refinement with phenix.refine[22] continued until R_{work} and R_{free} converged. Model quality was validated using COOT and MolProbity[23] prior to deposition in the Protein Data Bank with accession codes 4YL5 (apo) and 4YWR (PLP-bound). Diffraction images are available on Integrated Resource for Reproducibility in Macromolecular Crystallography (http://www.proteindiffraction.org).[24]

Structure Preparation, Ligand Selection, and Docking. The AbHMPK model was prepared for docking using well-established DOCK6 protocols.[25,26] Briefly, the coordinates of the protein (PDB ID: 4YWR) and the PLP reference ligand were saved separately in the MOL2 format. Hydrogens and charges were added to the protein and reference ligand using the AMBER ff14SB force field.[27] Subsequently, the protein molecular surface was generated by using the dms program, and then spheres were generated over the surface of the protein using the sphgen program. Spheres within 10 Å of the reference ligand were then selected. Following sphere generation, docking grids were generated using the grid function of DOCK6.[25] The ligands HMP (ZINC ID: 895559), HMPP (ZINC ID: 1529994), pyridoxal (ZINC ID: 120249) and PLP (ZINC ID: 1532514) were downloaded from the ZINC 15 database.[28,29] Each molecule was docked to the 4YWR energy grids using both rigid and flexible docking with DOCK6. The grid scores for the docked molecules are given in Table S1.

ATPase Assay. A coupled enzyme assay was used for measuring AbHMPK activity by coupling the production of ADP to the production of NADH, measured spectrophotometrically at 340 nm. Initially, a 2x ATPase buffer was prepared with 25 mM HEPES, pH 7.5, and 150 mM NaCl, containing 2 mM phosphoenolpyruvate (PEP, Sigma-Aldrich), 25 units of

https://doi.org/10.1021/acs.biochem.3c00640
Biochemistry XXXX, XXX, XXX−XXX

pyruvate kinase (PK, Sigma-Aldrich) and lactate dehydrogenase (LDH, Sigma-Aldrich), and 400 μM $MgCl_2$. The assay was run by combining 1× ATPase buffer, 500 μM NADH (GoldBio), 2 mM ATP (Fisher), enzyme, and the compound to be tested. The activity of AbHMPK was tested by varying the concentration of three different compounds: (4-Amino-2-methylpyrimidin-5-yl) methanol hydrochloride (HMP, AmBeed), 3-Hydroxy-5-(hydroxymethyl)-2-methylisonicotinaldehyde hydrochloride (Pyridoxal, AmBeed), and 4-Formyl-5-hydroxy-6-methylpyridin-3-yl methyl dihydrogen phosphate (PLP, AmBeed). The enzyme was used at a final concentration of approximately 0.3 mg/mL in a 100 μL reaction (1 nmol of enzyme per reaction). The assay was initiated by the addition of enzyme (for kinetics) or substrate (for dose response) and monitored at 340 nm on a SpectraMax M2 multimode microplate reader (Molecular Devices).

HPLC Analysis. The AbHMPK reaction was run as described above in the ATPase Assay section, and reactions were quenched by placing the tubes at 95 °C for 2 min. To confirm that the substrates and products were stable under the quenching conditions, a parallel set of reactions was run where the reaction was stopped by passing the reaction mixture through a 10,000 MWCO centricon (Millipore). No difference between the two approaches was observed. The quenched samples were analyzed by HPLC (Agilent 1100 series) with a 4.6 mm × 250 mm BioSAX NP5. SS column (Agilent) running a gradient of 8−30% of 1 M ammonium bicarbonate, pH 8.0, in water over 30 min. Standards of HMP, ADP, and ATP were run separately and added to a standard run (spiked), to confirm their elution times. The single observed product was confirmed by UV and LC-MS/MS.

LC-MS/MS Analysis. As the HPLC analysis of the HMPK-catalyzed reaction used a method that is not compatible with MS/MS, the product peak from HPLC (as described in the previous section) was collected, diluted with water, and further analyzed. The LC-MS and MS/MS analysis was performed on a 6460C triple quad mass spectrometer (Agilent) with an inline 1290 LC system (Agilent). The HMP standard or the reaction product, dissolved in 10% acetonitrile and 90% water, was directly injected without using a column. The mass of the parent ion was first established by doing a parent ion scan from 50−500 Da, with a scan time of 50, a fragmentor voltage of 100 V, and a cell accelerator voltage of 4 eV. This was followed by a product ion scan from 25 to 250 Da using a scan time of 50, a fragmentor voltage of 135 V, and a cell accelerator voltage of 4 eV. For all experiments, the mass spectrometer used an ion source temperature of 250 °C, sheath gas temperature of 350 °C, nebulizer pressure of 45 psi, nozzle voltage of 1.5 kV, and capillary current of 3500 nA. Data was analyzed and spectra were generated using MassHunter Qualitative Analysis software.

Steady-State Enzyme Kinetics. The ATPase assay, described above, was used to measure the initial reaction rate (before 10% completion) at substrate concentrations ranging from 10 μM to 2 mM. Triplicate independent experiments were carried out, and the values for the mean ± standard error were plotted for each ligand concentration tested. The data was then fit using the Michaelis−Menten equation, and values for K_M, and V_{max} were derived from this fit (KaleidaGraph, Synergy Software). The value of k_{cat} was determined by dividing the computed V_{max} by the concentration of the enzyme in the reaction (10 μM).

Dose−Response Curve for PLP. Inhibition of AbHMPK was determined using the ATPase assay described above. The enzyme was first mixed with ATPase buffer, NADH, ATP, and enzyme, and incubated for 10 min before initiating the reaction with the addition of 100 μM (final concentration) of HMP. Initial rates of the reaction were determined from the progress curves for each PLP concentration tested. The data was converted to % activity by dividing each value by the rate of the reaction in the absence of PLP. The resulting data was plotted against PLP concentration on a log scale and fit with a 4-point sigmoidal curve (KaleidaGraph, Synergy Software):

$$\%\,\text{activity} = \frac{\text{max}}{\text{min} + (\text{IC}_{50}/[I])^h}$$

Where $[I]$ = the inhibitor concentration, max = maximum % activity, min = minimum % activity, h = hill slope, and IC_{50} = concentration at the inflection point (50% activity).

RESULTS AND DISCUSSION

Protein Expression, Purification, and Structure Solution. The putative HMPK from *A. baumannii* IS-123 (903899) was expressed and purified to homogeneity using established methods.[17−19] After sparse matrix screening using sitting drop crystallization, diffraction-quality crystals were obtained in a solution containing 200 mM ammonium sulfate, 100 mM sodium citrate, pH 5.6, and 25% PEG 4000. To obtain the PLP-bound structure, crystals were soaked in this solution supplemented with 5 mM PLP. Both unliganded and PLP-soaked crystals were flash frozen in liquid nitrogen prior to data collection. Data collection statistics are given in Table 1. The crystals diffracted to high resolution (1.7 Å for apo and 1.65 Å for PLP-bound) and were indexed in the orthorhombic space group $C222_1$. Both crystals had a solvent content of 52% and a Matthews coefficient of 2.55. The structures were solved by molecular replacement using the *Staphylococcus aureus* pyridoxal kinase structure (4C5L)[16] as a search model. The structures refined to R_{work}/R_{free} values of 16.0/17.7% and 15.7/17.6% for the apo and PLP-bound structures, respectively. The data refinement statistics are listed in Table 1.

Structure of *A. baumannii* HMP Kinase. Based on sequence similarity, AbHMPK belongs to the ribokinase-like superfamily and is annotated as a member of the HMP(P) Kinase (ThiD) family. The overall structure is an $\alpha\beta\alpha$ sandwich with the characteristic ribokinase-like 8-stranded β-sheet flanked by eight helices, three on one side and five on the other (Figure 2A). In the case of AbHMPK, there is an additional strand that extends this to a 9-stranded sheet (topology and secondary structure numbering are given in Figure S1). As in other ribokinase family proteins, the active site is located in a groove sitting at the top of the β-sheet (Figure 2B). A structure search using the DALI server[30] against the protein data bank reveals primarily HMP kinases and the related pyridoxal kinases as having significant structural similarity (Table 2).

Despite the high degree of structural similarity among members of the ribokinase-like superfamily, the level of multimerization is varied and includes some that are monomers (adenosine kinase), dimers (ribokinase) or trimers (THZ kinase).[38−40] Similar to the previously reported HMPK enzymes, the observed overall AbHMPK structure is an elongated dimer (Figure 2C). This is consistent with the probable assembly reported by PDBePISA.[41] Analysis of the

https://doi.org/10.1021/acs.biochem.3c00640
Biochemistry XXXX, XXX, XXX−XXX

Table 1. Data Collection and Refinement Statistics

	AbHMPK	AbHMPK + PLP
Data Collection		
PDB ID	4YL5	4YWR
beamline	21-ID-G	NA (rotating anode)
detector	RAYONIX MX-300	RIGAKU Saturn 944+
wavelength (Å)	0.97856	1.5418
resolution range (Å)	29.41−1.70 (1.74−1.70)	46.18−1.65 (1.69−1.65)
space group	$C222_1$	$C222_1$
unit cell dimensions		
a, *b*, *c* (Å)	58.82, 108.10, 88.88	58.88, 108.10, 88.80
no. of measured reflections	141,847 (6037)	588,563 (11,540)
no. of unique reflections	31,307 (2162)	34,659 (2514)
mean $I/\sigma(I)$[a]	23.94 (2.39)	48.64 (3.81)
completeness (%)	99.2 (92.6)	99.7 (98.8)
redundancy	4.5 (3.8)	16.9 (4.6)
R_{merge} (%)	3.7 (40.9)	4.4 (48.7)
Data Refinement		
total no. of reflections	31,294 (2286)	34,354 (2445)
test set	1647 (143)	1802 (136)
R_{work}/R_{free} (%)	16.0/17.7	15.7/17.6
total no. of atoms	1906	1996
no. of ligand atoms	8	32
no. of waters	187	240
RMSD		
bonds (Å)	0.007	0.006
angles (deg)	1.071	0.838
mean *B* factor (Å^2)	28.54	21.19
Ramachandran plot (%)		
favored	99	100
allowed	1	0
outliers	0	0
MolProbity Clashscore (%)	2	2

[a]Values in parentheses represent the highest resolution shell.

dimer reveals a buried surface area of 3430 Å^2, more than 20% of the total surface area of 17,060 Å^2. The interface is composed of residues from two β-strands (β2 and β3, Figure S1) and two α-helices (α1 and α2, Figure S1) from each protomer that make extensive hydrogen bonding and hydrophobic interactions.

Active Site Architecture of AbHMPK. Each AbHMPK protomer contains one active site that is located near the dimer interface but composed entirely of residues from a single protomer. To identify ligand binding interactions, we conducted crystal-soaking experiments with several potential ligands, including HMP and pyridoxal derivatives. Upon soaking with pyridoxal 5′-phosphate (PLP), we obtained a high-resolution structure of PLP noncovalently bound to AbHMPK (Figure 3A,B). Overall, the secondary structures of liganded AbHMPK and unliganded AbHMPK are quite similar (Figure S2, RMSD of 0.120 Å). The ligand-bound structure illustrates the architecture of the active site and the residues that are putatively involved in binding to the substrate of this enzyme (Figure 3C). Previous structures of HMPK have identified a glutamate residue (E44 in *Salmonella typhimurium*) that hydrogen bonds with the 4-amino group of HMP to help orient this ligand in the active site.[7] In AbHMPK, Q51 plays this role, making hydrogen bonds with the 3-hydroxyl and 4-aldehyde groups (Figure 3C). This is consistent with a sequence comparison of HMPK enzymes, illustrating that the residue in this position is conserved as a glutamate or glutamine (Figure S3). Interestingly, the pyridoxal kinase from *Bacillus subtilis* has a methionine at this position, which may assist with the substrate specificity. The active site forms a cavity in the protein (Figure 2B) formed predominantly by several hydrophobic residues, including A25, M87, V114, A117, and L123. The side chains of N118 and highly conserved D112 (Figure S3) make additional hydrogen bonds with the phosphate of the ligand (Figure 3C). Note that in the AbHMPK structure with PLP bound, we observed two alternate conformations for the ligand (Figure 3C).

Unlike the *S. typhimurium* HMPK, which has an unstructured loop region that becomes ordered and acts as a lid for the active site when the substrate is bound, the structures of the active sites of unliganded and PLP-bound AbHMPK are very similar (Figure 4A).[7] Superposition of the HMP-bound *S. typhimurium* protein structure on AbHMPK (Figure 4B) illustrates the putative positioning of the native ligand, HMP. As expected, the pyridine ring lies in the same orientation as the pyridine ring of PLP and is situated in hydrogen bond distance with Q51 of AbHMPK. While a nucleotide-bound structure of an HMPK enzyme has not yet been reported, structures have been solved of pyridoxal kinases with bound ADP and ATP.[15,42] Using these structures as a guide, we identified the putative nucleotide binding site in AbHMPK (Figure 4C). As expected, the γ-phosphate of ATP is situated in a position to be added to the hydroxyl of HMP. These structures also provide insights as to why this enzyme does not accept pyridoxal as a substrate. The pyridoxal substrate binds in a slightly different orientation than that of HMP (Figure 4B), which would likely cause steric clashes with

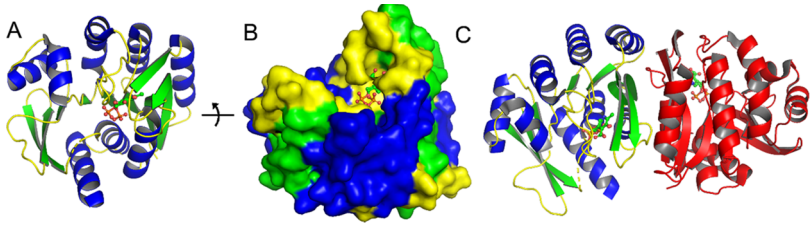

Figure 2. Overall structure of AbHMPK. AbHMPK has the characteristic ribokinase-like $\alpha\beta\alpha$ sandwich (A) with the active site buried in a cavity of the protein at the edge of the β-sheet (B). The active form of AbHMPK is an elongated dimer (C). In all panels, the PLP ligand soaked into crystals of AbHMPK is shown (ball-and-stick representation) to mark the active site. In this figure, α-helices are shown as blue ribbons, β-strands are shown as green arrows, and loops are shown in yellow, except in (C) which also shows one protomer completely in red. The surface diagram in (B) uses the same coloring scheme.

https://doi.org/10.1021/acs.biochem.3c00640
Biochemistry XXXX, XXX, XXX−XXX

Table 2. Results of DALI Search Using the Structure of AbHMPK

PDB ID	Z-score[a]	RMSD[b]	% ID[c]	description	ref.[d]
4JJP	28.9	1.7	33	phosphomethylpyrimidine kinase	TBP
1UB0	28.0	1.8	35	phosphomethylpyrimidine kinase	TBP
2I5B	27.1	2.0	26	phosphomethylpyrimidine kinase	15
4C5L	26.8	2.1	28	phosphomethylpyrimidine kinase	16
3RM5	26.7	2.0	32	phosphomethylpyrimidine kinase	9
1JXI	26.5	1.9	33	phosphomethylpyrimidine kinase	7
5ZWA	24.3	2.6	22	pyridoxine/pyridoxal kinase	31
1VI9	24.0	2.7	19	pyridoxamine kinase	32
1TD2	23.6	2.7	19	pyridoxamine kinase	33
3MBH	23.3	2.8	23	putative phosphomethylpyrimidine kinase	TBP
2DDM	23.2	2.7	26	pyridoxine kinase	34
6K8Z	23.1	2.6	19	pyridxoal kinase, putative	35
4S1M	22.9	2.9	20	pyridoxal kinase	36
5B6A	22.6	2.7	20	pyridoxal kinase PDXY	37
3PZS	22.0	3.0	20	pyridoxamine kinase	TBP

[a]The DALI Z-score is an optimized similarity score defined as the sum of equivalent residue-wise $C_\alpha - C_\alpha$ distances among two proteins.[30] [b]RMSD is the root-mean-square deviation in Å. [c]% ID is the percentage sequence identity between AbHMPK and the listed protein. [d]Reference. TBP = to be published.

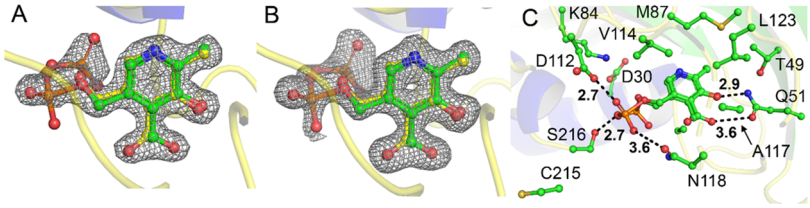

Figure 3. AbHMPK active site and ligand binding. Clear electron density was seen in the structure of the PLP bound in the active site. Both a composite omit map (A) and a difference ($F_O - F_C$) map (B) can fit well with PLP. The ligand was modeled in two conformations that were refined to nearly identical occupancies (49 and 51%). The active site of AbHMPK with the two conformations of PLP modeled (C) shows a similar organization as other HMPK enzymes. Hydrogen bonds are shown as dashed lines and distances are given in Å. In this figure, the amino acid side chains and PLP ligand are shown in ball-and-stick representation with the carbon atoms colored green, nitrogen atoms colored blue, oxygen atoms colored red, sulfur atoms colored yellow, and phosphorus atoms colored orange.

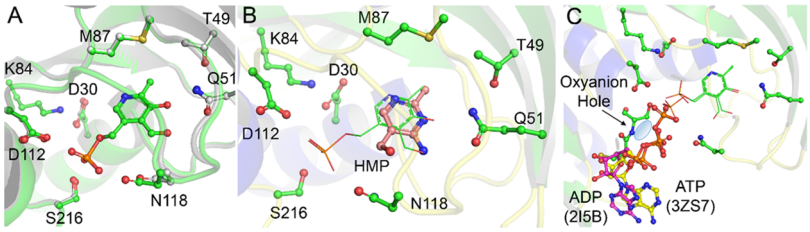

Figure 4. AbHMPK ligand binding. A superposition of unliganded and PLP-bound AbHMPK (A) reveals few differences (RMSD 0.120 Å). The position of the putative native ligand, HMP, was identified by superimposing the HMP-bound structure of *S. typhimurium* HMPK (1JX1) on the AbHMPK structure (B, HMP is shown with salmon-colored carbon atoms). Many of the hydrogen bonding interactions, particularly with Q51 and N118, are conserved. While no nucleotide-bound HMPK structures are available, superposition with the related pyridoxal kinases from *B. subtilis* (2I5B, ADP shown with purple carbon atoms) and *T. brucei* (3ZS7, ATP shown with yellow carbon atoms) illustrates the putative nucleotide binding position (C). The position of the putative oxyanion hole is shown with a blue oval. In all panels, the AbHMPK structure is modeled with green carbon atoms. Note that only one of the two alternate conformations of PLP is shown in parts (A) and (B), while both are shown in (C).

the incoming γ-phosphate of ATP (Figure 4C). The highly conserved GT/SGC motif that makes up the putative oxyanion hole (GSGC 212−215 in AbHMPK) is on an unstructured loop in AbHMPK and only C215 is observed in the structure (Figure 3C). This residue and C203 form a disulfide bond in the AbHMPK structure (Figure S4), causing C215 to point away from the putative site of the oxyanion hole. This disulfide is possibly an artifact of the purification and crystallization conditions. However, as it is adjacent to the conserved GSGC of the oxyanion hole, this disulfide may help to orient the backbone amides toward the oxanion intermediate (Figures 4C and S4). The flexibility of this motif, located on a solvent-exposed loop region, also suggests that there may be some plasticity inherent in the structure of the oxyanion pocket.

Docking Study of Potential AbHMPK Substrates and Products. The structure of HMP and pyridoxal are quite similar, and bifunctional enzymes that can turn over either substrate have been identified.[8,15,16] To further investigate the features of the active site that dictate substrate binding, we carried out docking studies using both HMP and pyridoxal, as well as their reaction products, HMP-P and PLP. After preparing the receptor (AbHMPK) and ligands (see Materials

https://doi.org/10.1021/acs.biochem.3c00640
Biochemistry XXXX, XXX, XXX−XXX

and Methods section), we used Dock6[25] to identify putative low-energy binding poses of the ligands in the active site. The docked HMP ligand (Figure S5A) showed a similar orientation as the known binding mode (Figure 4B), and pyridoxal (Figure S5B) was observed in the same position but flipped relative to what would be expected from the AbHMPK-PLP structure. The products, HMP-P and PLP, were also observed in similar positions and orientations but were also not consistent with the AbHMPK-PLP structure. This is likely due to limitations of the model, which lacked water molecules or the ATP cosubstrate, and was likely driven by interactions with the phosphate group of these ligands. While the results of the docking suggest that HMP, and the product HMP-P, make slightly more favorable interactions with AbHMPK than pyridoxal and PLP (Table S1), the difference is small and the ligands make many of the same interactions (Figure S5). Taken together with the structural data, these results suggest that this protein could accommodate either HMP or pyridoxal as a substrate.

Kinetics of AbHMPK Activity. Because of the similarity between HMPK and Pyridoxal kinase and the observed similar binding poses in our docking studies, we investigated the activity of AbHMPK for both HMP and pyridoxal using an ATPase assay. We tested the enzyme for its capacity to turn over HMP and pyridoxal as well as two structurally similar forms, pyridoxamine and pyridoxine. Interestingly, no reaction was observed when pyridoxal, pyridoxamine, or pyridoxine were used as cosubstrates. Similarly, when tested in the reverse direction, PLP did not turn over, ruling out the potential phosphatase activity of this enzyme. For HMP, however, the enzyme exhibited saturable kinetics, similar to other HMPK enzymes (Figure 5A).[8,43,44] Surprisingly, when we quantified the stoichiometry of the reaction, we determined that only one equivalent of ATP was used during the reaction (Figure 5B). This suggests that this enzyme catalyzes the single phosphorylation of HMP to HMP-P. To confirm this, we analyzed the reaction with HPLC (ion exchange) and LC-MS/MS. The reaction proceeds as expected, with a time-dependent decrease in the amount of substrate accompanied by the production of ADP from ATP. However, only a single product peak is observed, even when the reaction is allowed to proceed for 10 h (Figure 6). The elution time of the product is consistent with that of the monophosphate product, HMP-P, and the absorbance spectrum of the product peak matches exactly that of the HMP substrate (Figure S6). In addition, we analyzed the compound using LC-MS and confirmed that the product had a mass-to-charge (M/Z) of 220 (M+2, positive ion mode), consistent with HMP-P (Figure S7A,C). A product ion scan of the presumed HMP-P showed a set of product ions similar to that of the HMP standard (Figure S7B,D). While we cannot rule out the possibility that a diphosphate product is being produced and is rapidly degrading, HMP-PP has previously been shown to be isolable and amenable to HPLC analysis.[45,46] In addition, if this were the case, we would expect that two equiv of ATP would be consumed during the reaction.

Inhibition of AbHMPK Activity by PLP. While our activity data clearly show that AbHMPK has HMP kinase activity and likely serves this role in physiological contexts, the structure data clearly indicate that the PLP molecule can occupy the binding site (Figure 3). This might indicate that, while pyridoxal or PLP may not be native substrates, PLP could bind competitively and inhibit the enzyme. We measured

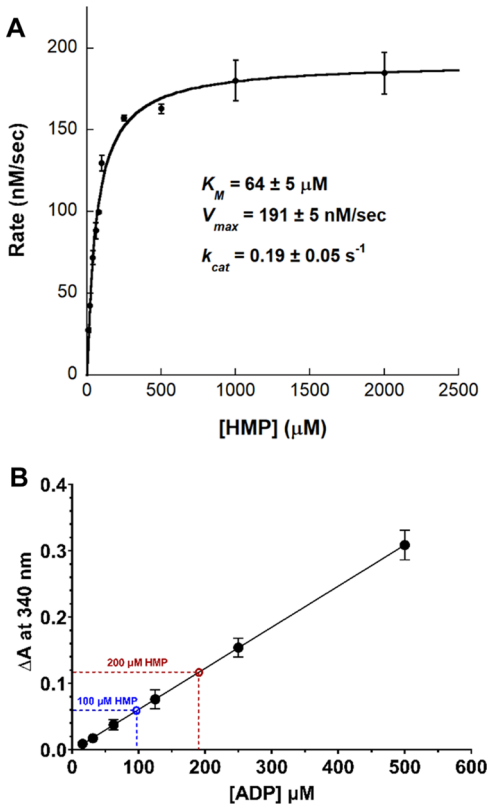

Figure 5. AbHMPK enzyme activity. The protein shows saturable kinetics with HMP as a substrate (A). The activity was measured with an ATPase assay. Using several concentrations of ADP to generate a standard curve, we determined that only one equivalent of ATP is consumed during the reaction (B).

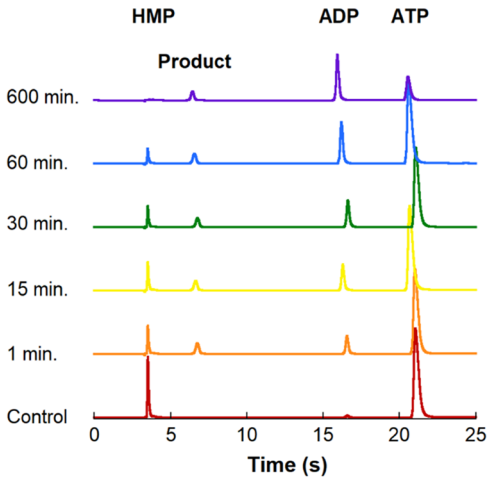

Figure 6. HPLC analysis of the AbHMPK activity. Consistent with the observation that this enzyme only uses one equivalent of ATP, the AbHMPK-catalyzed reaction appears to produce a single product. Analysis of the time course using ion-exchange chromatography (monitored at 260 nm) shows the disappearance of the substrates (HMP and ATP) and the appearance of ADP and a single product. The retention time of the product, the absorbance spectrum, and the mass spectrometry analysis all confirm that this single product is HMP-P. The control reaction (red) was run for 60 min in the absence of an enzyme. HMP, ADP, and ATP all have identical retention times and absorbance spectra as authentic standards.

https://doi.org/10.1021/acs.biochem.3c00640
Biochemistry XXXX, XXX, XXX−XXX

the kinetics of AbHMPK at increasing concentrations of PLP and determined that it does act as an inhibitor (Figure 7). A fit

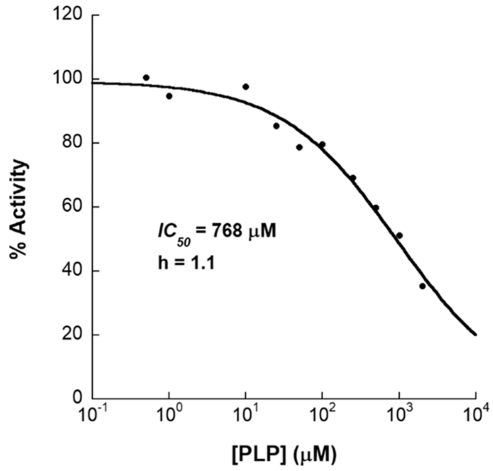

Figure 7. Inhibition of AbHMPK by PLP. While neither pyridoxal nor PLP are substrates of AbHMPK, PLP inhibits the enzyme at high micromolar concentrations. The data was fit using a 4-parameter sigmoidal dose−response curve.

to the data with a 4-parameter sigmoidal dose−response curve yielded an IC_{50} value of 768 μM with a hill coefficient of 1.1. While not a potent inhibitor, this suggests that PLP could potentially regulate the activity of this enzyme. PLP has been shown to similarly act as an inhibitor of pyridoxal kinase in *E. coli*.[47] In this case, however, it was determined to form a Schiff base with the enzyme, which is not observed in the structure of AbHMPK.

Herein we describe the structures of a putative HMPK enzyme from *A. baumannii* in both an unliganded and a PLP-bound state. The overall structure and active site architecture are similar to other known ribokinase-like family members. While the protein was initially identified as an HMPK by sequence comparison, our docking studies and cocrystal structure with PLP suggested that the protein may be a bifunctional HMPK/pyridoxal kinase. Enzyme kinetics, however, confirmed that this enzyme catalyzed the phosphorylation of HMP but did not turn over pyridoxal or related substrates. However, PLP does inhibit this enzyme with a high micromolar IC_{50}. While, to our knowledge, the intracellular PLP concentration has not been measured for *A. baumannii*, it has been reported to be in the low μm range in other microbes.[48,49] While likely not a major contributor to the regulation of thiamin biosynthesis, the inhibition of AbHMPK by PLP could be a potential regulatory mechanism in operation in *A. baumannii*. This mechanism of regulation may be in operation during times when PLP concentrations are abnormally high if the concentrations vary locally within the organism or are upregulated in response to changing environments. Co-regulation of thiamin and PLP biosynthesis has been previously reported in several contexts, including thiamin-dependent regulation of brain PLP in mammals, and the dependence on efficient PLP synthesis in yeast for thiamin biosynthesis.[50−54] This observation could also be explained by the enzymes involved in catalyzing the production of HMP-P and PLP having a common evolutionary ancestry. This explanation has been suggested to explain the presence of promiscuous kinases that can take HMP or pyridoxal as substrates.[11] Further studies are needed to fully describe the functional relevance of these observations.

Nearly all of the HMPK enzymes studied to date are bifunctional and catalyze both the phosphorylation of HMP and HMP-P.[4,7,10,45,55] The related PLK/HMPK class of enzymes is reported to catalyze the phosphorylation of pyridoxal or HMP but cannot add a second phosphate to HMP-P. Recent work on the evolution of HMPK and PLK enzymes indicates that these activities may have arisen from a common ancestral protein.[11,56] In fact, an engineered protein that was designed to represent the closest common ancestor between the ThiD/HMPKK and PLK/HMPK class is the most sequence-similar protein (to AbHMPK) with a solved structure (36% sequence identity).[56] The kinetics of AbHMPK indicate that this protein may occupy a distinct evolutionary niche between PLK/HMPPK-like and HMPPK/ThiD enzymes. The activity of AbHMPK as a monofunctional kinase that does not generate HMP-PP also raises an important question about this protein's role in thiamin biosynthesis. The biosynthesis of thiamin requires HMP-PP, which is combined with a thiazole phosphate to generate thiamine phosphate. While there are examples of monofunctional ThiD enzymes (ThiD2), they catalyze only the conversion of HMP-P to HMP-PP and can be putatively explained by alternative means of producing or importing HMP-P.[44] In the case of *A. baumannii*, an additional enzyme or alternative pathway must be present to generate the needed HMP-PP product from HMP-P.

A. baumannii, is one of the ESKAPE pathogens (*Enterococcus faecium*, *Staphylococcus aureus*, *Klebsiella pneumoniae*, *Acinetobacter baumannii*, *Pseudomonas aeruginosa*, and *Enterobacter* species) that are collectively the leading cause of nosocomial infections worldwide.[57,58] The biosynthesis of essential cofactors, such as thiamin, provides a largely untapped potential for targets for new antimicrobial drug candidates.[59−63] These data provide additional tools and insights to aid in the development of novel therapeutics that target the biosynthesis of thiamine in *A. baumannii* and related pathogens.

■ ASSOCIATED CONTENT

Data Availability Statement

The coordinate files and experimental data for the two structures described herein are freely available through the protein data bank (www.rcsb.org) with identifiers 4YL5 and 4YWR for the AbHMPK and AbHMPK-PLP structures, respectively.

Supporting Information

The Supporting Information is available free of charge at https://pubs.acs.org/doi/10.1021/acs.biochem.3c00640.

Additional figures and tables, including docking results, comparisons of structures, and spectroscopic characterization of the reaction product. Table S1. DOCK6 grid scores. Figure S1. Topology and secondary structure element number of AbHMPK. Figure S2. Comparison of liganded and unliganded AbHMPK. Figure S3. Sequence comparison of AbHMPK and related HMPK enzymes. Figure S4. Disulfide and oxyanion hole. Figure S5. Docking results. Figure S6. Absorbance spectrum of HMP standard and product of AbHMPK-catalyzed reaction. Figure S7. Mass analysis of HMP and product. (PDF)

https://doi.org/10.1021/acs.biochem.3c00640
Biochemistry XXXX, XXX, XXX−XXX

Accession Codes

The AbHMPK enzyme, described herein, is annotated in UniProt as A0A0J9X285 and A0A140UHE5 (100% sequence identity for these two records) as a putative phosphomethylpyrimidine kinase and a putative hydroxymethyl pyrimidine kinase/phosphomethylpyrimidine kinas, respectively.

■ AUTHOR INFORMATION

Corresponding Author

Jarrod B. French − *The Hormel Institute, University of Minnesota, Austin, Minnesota 55912, United States;* orcid.org/0000-0002-6762-1309; Phone: 507-437-9637; Email: jfremch@umn.edu

Authors

Humberto De Vitto − *The Hormel Institute, University of Minnesota, Austin, Minnesota 55912, United States;* Present Address: Van Cleve Cardiac Regenerative Medicine Program, Mayo Clinic Center for Regenerative Medicine, Rochester, Minnesota 55905, United States

Kafi Belfon − *Department of Biochemistry and Cell Biology, Stony Brook University, Stony Brook, New York 11790, United States;* orcid.org/0009-0003-9588-4290

Nandini Sharma − *The Hormel Institute, University of Minnesota, Austin, Minnesota 55912, United States;* orcid.org/0000-0003-4053-2186

Sarah Toay − *Department of Biological Chemistry, Grinnell College, Grinnell, Iowa 50112, United States*

Jan Abendroth − *UCB BioSciences, Bainbridge Island, Washington 98110, United States; Seattle Structural Genomics Center for Infectious Disease (SSGCID), Seattle, Washington 98104, United States*

David. M. Dranow − *UCB BioSciences, Bainbridge Island, Washington 98110, United States; Seattle Structural Genomics Center for Infectious Disease (SSGCID), Seattle, Washington 98104, United States*

Christine M. Lukacs − *UCB BioSciences, Bainbridge Island, Washington 98110, United States; Seattle Structural Genomics Center for Infectious Disease (SSGCID), Seattle, Washington 98104, United States*

Ryan Choi − *Seattle Structural Genomics Center for Infectious Disease (SSGCID), Seattle, Washington 98104, United States*

Hannah S. Udell − *Seattle Structural Genomics Center for Infectious Disease (SSGCID), Seattle, Washington 98104, United States*

Sydney Willis − *Department of Chemistry, Rollins College, Winter Park, Florida 32789, United States*

George Barrera − *Department of Chemistry and Biochemistry, Weber State University, Ogden, Utah 84408, United States*

Olive Beyer − *Department of Chemistry and Biochemistry, University of Maryland, Baltimore County, Baltimore, Maryland 21250, United States*

Teng Da Li − *Department of Biochemistry and Cell Biology, Stony Brook University, Stony Brook, New York 11790, United States*

Katherine A. Hicks − *Chemistry Department, SUNY Cortland, Cortland, New York 13045, United States;* orcid.org/0000-0002-1474-1067

Andrew T. Torelli − *Department of Chemistry, Ithaca College, Ithaca, New York 14850, United States;* orcid.org/0000-0003-4130-9867

Complete contact information is available at: https://pubs.acs.org/10.1021/acs.biochem.3c00640

Author Contributions

⋈H.D.V. and K.B. contributed equally.

Funding

This work was supported in part by the National Institutes of General Medical Sciences, and the National Institute of Allergy and Infectious Diseases, of the National Institutes of Health, Department of Health and Human Services, under Grant Number R35GM124898 (J.B.F.) and under Contract Nos.: 75N93022C00036, HHSN272201700059C, HHSN272201200025C, and HHSN272200700057C (SSGCID). This research used resources of the Advanced Photon Source, a U.S. Department of Energy (DOE) Office of Science User Facility operated for the DOE Office of Science by Argonne National Laboratory under Contract No. DE-AC02-06CH11357. Use of the LS-CAT Sector 21 was supported by the Michigan Economic Development Corporation and the Michigan Technology Tri-Corridor (Grant 085P1000817). In addition, parts of this work were conducted by students in the Molecular Interactions Virtual REU program, supported by the National Science Foundation under Grant Numbers 2149978 (J.B.F., K.A.H., A.T.T.) and 2042704 (J.B.F.). The funding agencies did not play a role in the conception, implementation, or analysis of the research described.

Notes

The authors declare no competing financial interest.

■ REFERENCES

(1) Bettendorff, L.; Wins, P. Thiamin diphosphate in biological chemistry: new aspects of thiamin metabolism, especially triphosphate derivatives acting other than as cofactors. *FEBS J.* **2009**, *276*, 2917−2925.

(2) Whitfield, K. C.; Bourassa, M. W.; Adamolekun, B.; Bergeron, G.; Bettendorff, L.; Brown, K. H.; Cox, L.; Fattal-Valevski, A.; Fischer, P. R.; Frank, E. L.; Hiffler, L.; Hlaing, L. M.; Jefferds, M. E.; Kapner, H.; Kounnavong, S.; Mousavi, M. P. S.; Roth, D. E.; Tsaloglou, M. N.; Wieringa, F.; Combs, G. F., Jr. Thiamine deficiency disorders: diagnosis, prevalence, and a roadmap for global control programs. *Ann. N. Y. Acad. Sci.* **2018**, *1430*, 3−43.

(3) Jurgenson, C. T.; Begley, T. P.; Ealick, S. E. The structural and biochemical foundations of thiamin biosynthesis. *Annu. Rev. Biochem.* **2009**, *78*, 569−603.

(4) Begley, T. P.; Downs, D. M.; Ealick, S. E.; McLafferty, F. W.; Van Loon, A. P.; Taylor, S.; Campobasso, N.; Chiu, H. J.; Kinsland, C.; Reddick, J. J.; Xi, J. Thiamin biosynthesis in prokaryotes. *Arch. Microbiol.* **1999**, *171*, 293−300.

(5) Begley, T. P.; Ealick, S. E.; McLafferty, F. W. Thiamin biosynthesis: still yielding fascinating biological chemistry. *Biochem. Soc. Trans.* **2012**, *40*, 555−560.

(6) Jurgenson, C. T.; Ealick, S. E.; Begley, T. P. Biosynthesis of Thiamin Pyrophosphate. *EcoSal Plus* **2009**, *3*, No. e7, DOI: 10.1128/ecosalplus.3.6.3.7.

(7) Cheng, G.; Bennett, E. M.; Begley, T. P.; Ealick, S. E. Crystal structure of 4-amino-5-hydroxymethyl-2-methylpyrimidine phosphate kinase from Salmonella typhimurium at 2.3 A resolution. *Structure* **2002**, *10*, 225−235.

(8) Cea, P. A.; Araya, G.; Vallejos, G.; Recabarren, R.; Alzate-Morales, J.; Babul, J.; Guixe, V.; Castro-Fernandez, V. Characterization of hydroxymethylpyrimidine phosphate kinase from mesophilic and thermophilic bacteria and structural insights into their differential thermal stability. *Arch. Biochem. Biophys.* **2020**, *688*, No. 108389.

(9) French, J. B.; Begley, T. P.; Ealick, S. E. Structure of trifunctional THI20 from yeast. *Acta Crystallogr., Sect. D* **2011**, *67*, 784−791.

(10) Kawasaki, Y.; Onozuka, M.; Mizote, T.; Nosaka, K. Biosynthesis of hydroxymethylpyrimidine pyrophosphate in Saccharomyces cerevisiae. *Curr. Genet.* **2005**, *47*, 156−162.

(11) Castro-Fernandez, V.; Bravo-Moraga, F.; Ramirez-Sarmiento, C. A.; Guixe, V. Emergence of pyridoxal phosphorylation through a promiscuous ancestor during the evolution of hydroxymethyl pyrimidine kinases. *FEBS Lett.* **2014**, *588*, 3068−3073.

(12) Li, M. H.; Kwok, F.; Chang, W. R.; Lau, C. K.; Zhang, J. P.; Lo, S. C.; Jiang, T.; Liang, D. C. Crystal structure of brain pyridoxal kinase, a novel member of the ribokinase superfamily. *J. Biol. Chem.* **2002**, *277*, 46385−46390.

(13) McCormick, D. B.; Gregory, M. E.; Snell, E. E. Pyridoxal phosphokinases. I. Assay, distribution, purification, and properties. *J. Biol. Chem.* **1961**, *236*, 2076−2084.

(14) Park, J. H.; Burns, K.; Kinsland, C.; Begley, T. P. Characterization of two kinases involved in thiamine pyrophosphate and pyridoxal phosphate biosynthesis in Bacillus subtilis: 4-amino-5-hydroxymethyl-2methylpyrimidine kinase and pyridoxal kinase. *J. Bacteriol.* **2004**, *186*, 1571−1573.

(15) Newman, J. A.; Das, S. K.; Sedelnikova, S. E.; Rice, D. W. The crystal structure of an ADP complex of Bacillus subtilis pyridoxal kinase provides evidence for the parallel emergence of enzyme activity during evolution. *J. Mol. Biol.* **2006**, *363*, 520−530.

(16) Nodwell, M. B.; Koch, M. F.; Alte, F.; Schneider, S.; Sieber, S. A. A subfamily of bacterial ribokinases utilizes a hemithioacetal for pyridoxal phosphate salvage. *J. Am. Chem. Soc.* **2014**, *136*, 4992−4999.

(17) Bryan, C. M.; Bhandari, J.; Napuli, A. J.; Leibly, D. J.; Choi, R.; Kelley, A.; Van Voorhis, W. C.; Edwards, T. E.; Stewart, L. J. High-throughput protein production and purification at the Seattle Structural Genomics Center for Infectious Disease. *Acta Crystallogr., Sect. F* **2011**, *67*, 1010−1014.

(18) Choi, R.; Kelley, A.; Leibly, D.; Hewitt, S. N.; Napuli, A.; Van Voorhis, W. Immobilized metal-affinity chromatography protein-recovery screening is predictive of crystallographic structure success. *Acta Crystallogr., Sect. F* **2011**, *67*, 998−1005.

(19) Serbzhinskiy, D. A.; Clifton, M. C.; Sankaran, B.; Staker, B. L.; Edwards, T. E.; Myler, P. J. Structure of an ADP-ribosylation factor, ARF1, from Entamoeba histolytica bound to Mg(2+)-GDP. *Acta Crystallogr., Sect. F* **2015**, *71*, 594−599.

(20) Aslanidis, C.; de Jong, P. J. Ligation-independent cloning of PCR products (LIC-PCR). *Nucleic Acids Res.* **1990**, *18*, 6069−6074.

(21) Emsley, P.; Cowtan, K. Coot: model-building tools for molecular graphics. *Acta Crystallogr., Sect. D* **2004**, *60*, 2126−2132.

(22) Adams, P. D.; Afonine, P. V.; Bunkoczi, G.; Chen, V. B.; Echols, N.; Headd, J. J.; Hung, L. W.; Jain, S.; Kapral, G. J.; Grosse Kunstleve, R. W.; McCoy, A. J.; Moriarty, N. W.; Oeffner, R. D.; Read, R. J.; Richardson, D. C.; Richardson, J. S.; Terwilliger, T. C.; Zwart, P. H. The Phenix software for automated determination of macromolecular structures. *Methods* **2011**, *55*, 94−106.

(23) Chen, V. B.; Arendall, W. B., 3rd; Headd, J. J.; Keedy, D. A.; Immormino, R. M.; Kapral, G. J.; Murray, L. W.; Richardson, J. S.; Richardson, D. C. MolProbity: all-atom structure validation for macromolecular crystallography. *Acta Crystallogr., Sect. D* **2010**, *66*, 12−21.

(24) Grabowski, M.; Langner, K. M.; Cymborowski, M.; Porebski, P. J.; Sroka, P.; Zheng, H.; Cooper, D. R.; Zimmerman, M. D.; Elsliger, M. A.; Burley, S. K.; Minor, W. A public database of macromolecular diffraction experiments. *Acta Crystallogr., Sect. D* **2016**, *72*, 1181−1193.

(25) Allen, W. J.; Balius, T. E.; Mukherjee, S.; Brozell, S. R.; Moustakas, D. T.; Lang, P. T.; Case, D. A.; Kuntz, I. D.; Rizzo, R. C. DOCK 6: Impact of new features and current docking performance. *J. Comput. Chem.* **2015**, *36*, 1132−1156.

(26) Mukherjee, S.; Balius, T. E.; Rizzo, R. C. Docking validation resources: protein family and ligand flexibility experiments. *J. Chem. Inf. Model.* **2010**, *50*, 1986−2000.

(27) Maier, J. A.; Martinez, C.; Kasavajhala, K.; Wickstrom, L.; Hauser, K. E.; Simmerling, C. ff14SB: Improving the Accuracy of Protein Side Chain and Backbone Parameters from ff99SB. *J. Chem. Theory Comput.* **2015**, *11*, 3696−3713.

(28) Irwin, J. J.; Sterling, T.; Mysinger, M. M.; Bolstad, E. S.; Coleman, R. G. ZINC: a free tool to discover chemistry for biology. *J. Chem. Inf. Model.* **2012**, *52*, 1757−1768.

(29) Sterling, T.; Irwin, J. J. ZINC 15–Ligand Discovery for Everyone. *J. Chem. Inf. Model.* **2015**, *55*, 2324−2337.

(30) Holm, L. Dali server: structural unification of protein families. *Nucleic Acids Res.* **2022**, *50*, W210−W215.

(31) Deka, G.; Kalyani, J. N.; Jahangir, F. B.; Sabharwal, P.; Savithri, H. S.; Murthy, M. R. N. Structural and functional studies on Salmonella typhimurium pyridoxal kinase: the first structural evidence for the formation of Schiff base with the substrate. *FEBS J.* **2019**, *286*, 3684−3700.

(32) Badger, J.; Sauder, J. M.; Adams, J. M.; Antonysamy, S.; Bain, K.; Bergseid, M. G.; Buchanan, S. G.; Buchanan, M. D.; Batiyenko, Y.; Christopher, J. A.; Emtage, S.; Eroshkina, A.; Feil, I.; Furlong, E. B.; Gajiwala, K. S.; Gao, X.; He, D.; Hendle, J.; Huber, A.; Hoda, K.; Kearins, P.; Kissinger, C.; Laubert, B.; Lewis, H. A.; Lin, J.; Loomis, K.; Lorimer, D.; Louie, G.; Maletic, M.; Marsh, C. D.; Miller, I.; Molinari, J.; Muller-Dieckmann, H. J.; Newman, J. M.; Noland, B. W.; Pagarigan, B.; Park, F.; Peat, T. S.; Post, K. W.; Radojicic, S.; Ramos, A.; Romero, R.; Rutter, M. E.; Sanderson, W. E.; Schwinn, K. D.; Tresser, J.; Winhoven, J.; Wright, T. A.; Wu, L.; Xu, J.; Harris, T. J. Structural analysis of a set of proteins resulting from a bacterial genomics project. *Proteins* **2005**, *60*, 787−796.

(33) Safo, M. K.; Musayev, F. N.; Hunt, S.; di Salvo, M. L.; Scarsdale, N.; Schirch, V. Crystal structure of the PdxY Protein from *Escherichia coli*. *J. Bacteriol.* **2004**, *186*, 8074−8082.

(34) Safo, M. K.; Musayev, F. N.; di Salvo, M. L.; Hunt, S.; Claude, J. B.; Schirch, V. Crystal structure of pyridoxal kinase from the *Escherichia coli* pdxK gene: implications for the classification of pyridoxal kinases. *J. Bacteriol.* **2006**, *188*, 4542−4552.

(35) Are, S.; Gatreddi, S.; Jakkula, P.; Qureshi, I. A. Structural attributes and substrate specificity of pyridoxal kinase from Leishmania donovani. *Int. J. Biol. Macromol.* **2020**, *152*, 812−827.

(36) Tarique, K. F.; Devi, S.; Tomar, P.; Ali, M. F.; Rehman, S. A. A.; Gourinath, S. Characterization and functional insights into the Entamoeba histolytica pyridoxal kinase, an enzyme essential for its survival. *J. Struct. Biol.* **2020**, *212*, No. 107645.

(37) Kim, M. I.; Hong, M. Crystal structure and catalytic mechanism of pyridoxal kinase from Pseudomonas aeruginosa. *Biochem. Biophys. Res. Commun.* **2016**, *478*, 300−306.

(38) Campobasso, N.; Mathews, I. I.; Begley, T. P.; Ealick, S. E. Crystal structure of 4-methyl-5-beta-hydroxyethylthiazole kinase from Bacillus subtilis at 1.5 A resolution. *Biochemistry* **2000**, *39*, 7868−7877.

(39) Mathews, I. I.; Erion, M. D.; Ealick, S. E. Structure of human adenosine kinase at 1.5 A resolution. *Biochemistry* **1998**, *37*, 15607−15620.

(40) Sigrell, J. A.; Cameron, A. D.; Jones, T. A.; Mowbray, S. L. Structure of *Escherichia coli* ribokinase in complex with ribose and dinucleotide determined to 1.8 A resolution: insights into a new family of kinase structures. *Structure* **1998**, *6*, 183−193.

(41) Krissinel, E.; Henrick, K. Inference of macromolecular assemblies from crystalline state. *J. Mol. Biol.* **2007**, *372*, 774−797.

(42) Jones, D. C.; Alphey, M. S.; Wyllie, S.; Fairlamb, A. H. Chemical, genetic and structural assessment of pyridoxal kinase as a drug target in the African trypanosome. *Mol. Microbiol.* **2012**, *86*, 51−64.

(43) Reddick, J. J.; Nicewonger, R.; Begley, T. P. Mechanistic studies on thiamin phosphate synthase: evidence for a dissociative mechanism. *Biochemistry* **2001**, *40*, 10095−10102.

(44) Thamm, A. M.; Li, G.; Taja-Moreno, M.; Gerdes, S. Y.; de Crecy-Lagard, V.; Bruner, S. D.; Hanson, A. D. A strictly monofunctional bacterial hydroxymethylpyrimidine phosphate kinase precludes damaging errors in thiamin biosynthesis. *Biochem. J.* **2017**, *474*, 2887−2895.

https://doi.org/10.1021/acs.biochem.3c00640
Biochemistry XXXX, XXX, XXX−XXX

(45) Hayashi, M.; Kobayashi, K.; Esaki, H.; Konno, H.; Akaji, K.; Tazuya, K.; Yamada, K.; Nakabayashi, T.; Nosaka, K. Enzymatic and structural characterization of an archaeal thiamin phosphate synthase. *Biochim. Biophys. Acta* **2014**, *1844*, 803−809.

(46) Reddick, J. J.; Kinsland, C.; Nicewonger, R.; Christian, D. M.; Downs, M. E.; Winkler, M. E.; Begley, T. Overexpression, purification and characterization of two pyrimidine kinases involved in the biosynthesis of thiamine: 4-amino-5-hydroxymethyl-2-methylpyrimidine kinase and 4-amino-5-hydroxymethyl-2-methylpyrimidine phosphate kinase. *Tetrahedron* **1998**, *54*, 15983−15991.

(47) Ghatge, M. S.; Contestabile, R.; di Salvo, M. L.; Desai, J. V.; Gandhi, A. K.; Camara, C. M.; Florio, R.; Gonzalez, I. N.; Parroni, A.; Schirch, V.; Safo, M. K. Pyridoxal 5′-phosphate is a slow tight binding inhibitor of *E. coli* pyridoxal kinase. *PLoS One* **2012**, *7*, No. e41680.

(48) di Salvo, M. L.; Contestabile, R.; Safo, M. K. Vitamin B(6) salvage enzymes: mechanism, structure and regulation. *Biochim. Biophys. Acta* **2011**, *1814*, 1597−1608.

(49) Zhao, G.; Winkler, M. E. Kinetic limitation and cellular amount of pyridoxine (pyridoxamine) 5′-phosphate oxidase of *Escherichia coli* K-12. *J. Bacteriol.* **1995**, *177*, 883−891.

(50) Bunik, V.; Aleshin, V.; Nogues, I.; Kahne, T.; Parroni, A.; Contestabile, R.; Salvo, M. L.; Graf, A.; Tramonti, A. Thiamine-dependent regulation of mammalian brain pyridoxal kinase in vitro and in vivo. *J. Neurochem.* **2022**, *161*, 20−39.

(51) Lai, R. Y.; Huang, S.; Fenwick, M. K.; Hazra, A.; Zhang, Y.; Rajashankar, K.; Philmus, B.; Kinsland, C.; Sanders, J. M.; Ealick, S. E.; Begley, T. P. Thiamin pyrimidine biosynthesis in Candida albicans: a remarkable reaction between histidine and pyridoxal phosphate. *J. Am. Chem. Soc.* **2012**, *134*, 9157−9159.

(52) Mondal, A.; Lai, R. Y.; Fedoseyenko, D.; Giri, N.; Begley, T. P. Oxidative Dearomatization of PLP in Thiamin Pyrimidine Biosynthesis in Candida albicans. *J. Am. Chem. Soc.* **2023**, *145*, 4421−4430.

(53) Paxhia, M. D.; Downs, D. M. SNZ3 Encodes a PLP Synthase Involved in Thiamine Synthesis in Saccharomyces cerevisiae. *G3* **2019**, *9*, 335−344.

(54) Paxhia, M. D.; Downs, D. M. Pyridoxal and alpha-Ketoglutarate Independently Improve Function of Saccharomyces cerevisiae Thi5 in the Metabolic Network of Salmonella enterica. *J. Bacteriol.* **2022**, *204*, No. e00450-21, DOI: 10.1128/JB.00450-21.

(55) Mizote, T.; Tsuda, M.; Smith, D. D. S.; Nakayama, H.; Nakazawa, T. Cloning and characterization of the thiD/J gene of *Escherichia coli* encoding a thiamin-synthesizing bifunctional enzyme, hydroxymethylpyrimidine kinase/phosphomethylpyrimidine kinase. *Microbiology* **1999**, *145* (Pt 2), 495−501.

(56) Gonzalez-Ordenes, F.; Bravo-Moraga, F.; Gonzalez, E.; Hernandez-Cabello, L.; Alzate-Morales, J.; Guixe, V.; Castro-Fernandez, V. Crystal structure and molecular dynamics simulations of a promiscuous ancestor reveal residues and an epistatic interaction involved in substrate binding and catalysis in the ATP-dependent vitamin kinase family members. *Protein Sci.* **2021**, *30*, 842−854.

(57) Mulani, M. S.; Kamble, E. E.; Kumkar, S. N.; Tawre, M. S.; Pardesi, K. R. Emerging Strategies to Combat ESKAPE Pathogens in the Era of Antimicrobial Resistance: A Review. *Front. Microbiol.* **2019**, *10*, 539.

(58) Santajit, S.; Indrawattana, N. Mechanisms of Antimicrobial Resistance in ESKAPE Pathogens. *BioMed Res. Int.* **2016**, *2016*, No. 2475067.

(59) Drebes, J.; Kunz, M.; Windshugel, B.; Kikhney, A. G.; Muller, I. B.; Eberle, R. J.; Oberthur, D.; Cang, H.; Svergun, D. I.; Perbandt, M.; Betzel, C.; Wrenger, C. Structure of ThiM from Vitamin B1 biosynthetic pathway of Staphylococcus aureus - Insights into a novel pro-drug approach addressing MRSA infections. *Sci. Rep.* **2016**, *6*, No. 22871.

(60) Du, Q.; Wang, H.; Xie, J. Thiamin (vitamin B1) biosynthesis and regulation: a rich source of antimicrobial drug targets? *Int. J. Biol. Sci.* **2011**, *7*, 41−52.

(61) Kim, H. J.; Lee, H.; Lee, Y.; Choi, I.; Ko, Y.; Lee, S.; Jang, S. The ThiL enzyme is a valid antibacterial target essential for both thiamine biosynthesis and salvage pathways in Pseudomonas aeruginosa. *J. Biol. Chem.* **2020**, *295*, 10081−10091.

(62) von Pappenheim, F. R.; Aldeghi, M.; Shome, B.; Begley, T.; de Groot, B. L.; Tittmann, K. Structural basis for antibiotic action of the B(1) antivitamin 2′-methoxy-thiamine. *Nat. Chem. Biol.* **2020**, *16*, 1237−1245.

(63) Tillery, L. M.; Barrett, K. F.; Dranow, D. M.; Craig, J.; Shek, R.; Chun, I.; Barrett, L. K.; Phan, I. Q.; Subramanian, S.; Abendroth, J.; Lorimer, D. D.; Edwards, T. E.; Van Voorhis, W. C. Toward a structome of Acinetobacter baumannii drug targets. *Protein Sci.* **2020**, *29*, 789−802.